BRIGHTNESS VARIATIONS WITHIN LUNAR SHADOWS AS PERCEIVED BY ASTRONAUTS. R. V. Wagner, A. K. Boyd, P. Mahanti, and M. S. Robinson. Intuitive Machines, 101 E. Jackson St., Phoenix, AZ, 85004 (rwagner@intuitivemachines.com).

Introduction: The NASA ShadowCam instrument is a high-resolution camera onboard the Korea Pathfinder Lunar Orbiter (KPLO, or Danuri) designed to image in polar shadowed areas with a pixel scale of ~2 meters **[1]**. ShadowCam began regular orbital imaging in February 2023 and has acquired images over two cycles of seasonal lighting changes. ShadowCam images provide direct measurements of illumination levels (measured in radiance) inside permanent and temporary shadows, and we have previously shown that the lighting conditions in these shadows can be quite bright from a human perspective. At the high end, polar shadows can be as bright as a well-lit office space **[2]**.

This abstract expands on our previous work by investigating the range of brightness expected within a given large permanently shadowed region (PSR), both from the perspective of varying lighting across distance and from varying slope orientations and viewing angles.

Methods: We determine brightness within large PSRs by measuring median radiance (W/m^2/sr/µm) in a 600×600 m box centered on some point and then convert to luminance. We additionally record the season, local time-of-day, and other image metadata. We also measure the same value for 80 additional boxes in a 9×9 grid, centered at ~900 m intervals surrounding the original location (**Fig. 1**). Local time of day is a 24-unit location-independent measure of lighting direction (calculated as *(local longitude – sub-solar longitude) / 360 × 24*), where 12.0 is the Sun directly north or south (noon), 6.0 is nominally sunrise, and 18.0 is nominally sunset, though sunrise and sunset times vary considerably near the poles. Note that since longitude increments very rapidly with distance at the pole, we always calculate time of day using the location of the central point, so that a single Sun position gives the same time of day for all sample points in the PSR.

The ShadowCam minimum detectable signal is close to a radiance of ~0.0007 (approximately 0.05 cd/m^2, or –1.25 EV), depending on various imaging parameters. Scenes with >50% of pixels having radiance values below this level will be recorded as brighter than they actually are due to the instrument's minimum recorded value being higher than the scene should produce. In our plots, –1.25 EV is marked to indicate that lower values are likely too high.

Luminance: While ShadowCam is an excellent instrument for collecting accurate and precise radiance values, radiance is not a useful unit for determining the apparent brightness of a scene to a human without paying close attention to the wavelengths involved. ShadowCam has a strong response over its full wavelength range (410 nm to 780 nm), while human perceptual brightness is dominated by light from ~500-640 nm **[3,4]**. Fortunately, since solar spectral output, the ShadowCam response curve, and lunar regolith reflectance properties are roughly constant, we can use a fixed conversion factor to scale ShadowCam radiance values to luminance values for shadowed lunar scenes **[2]**.

We have updated our conversion factor from 71 **[2]** to 73 ($cd/m^2 = 73 \times W/m^2/sr/\mu m$) based on a more physically accurate treatment of the calculations. This 3% change does not alter our prior conclusions about overall brightness within PSRs, and is negligible relative to local variations in observed brightness (**Fig. 1**).

Exposure Value: A convenient derivative value of the luminance of a scene is Exposure Value (EV), a measure photographers use to determine optimal camera settings for a scene. An increase of 1 EV is ×2 cd/m^2, and for ISO 100, $EV = log_2(cd/m^2 \times 8)$ **[5]**. Above ~EV 4, we do not expect astronauts to need artificial light except possibly for close examination of samples; below ~EV 2, we expect them to want artificial light even for walking around. Offices well-lit by overhead lights are typically in the range of EV 6 to 8.

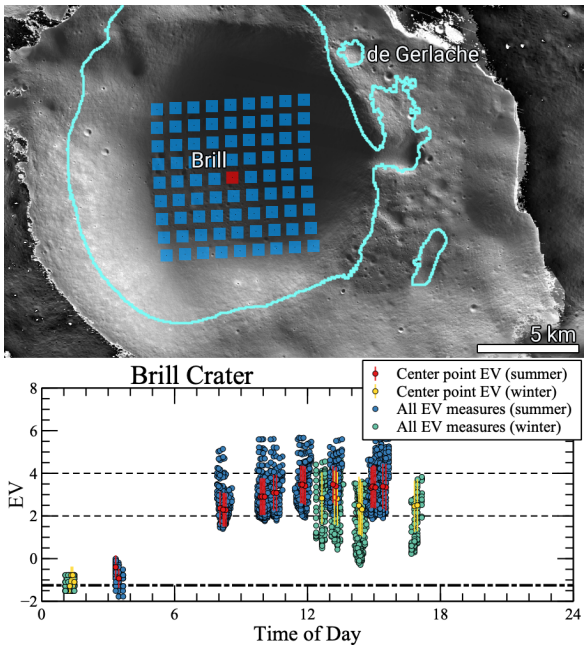

Figure 1: Example crater dataset. *Top:* Sampling regions (red and blue squares) in PSR (teal outline) in south polar crater Brill (88.3°S, 267°E). *Bottom:* Brightnesses in summer and winter. Uncertainty interval is standard deviation of all points at same time of day.

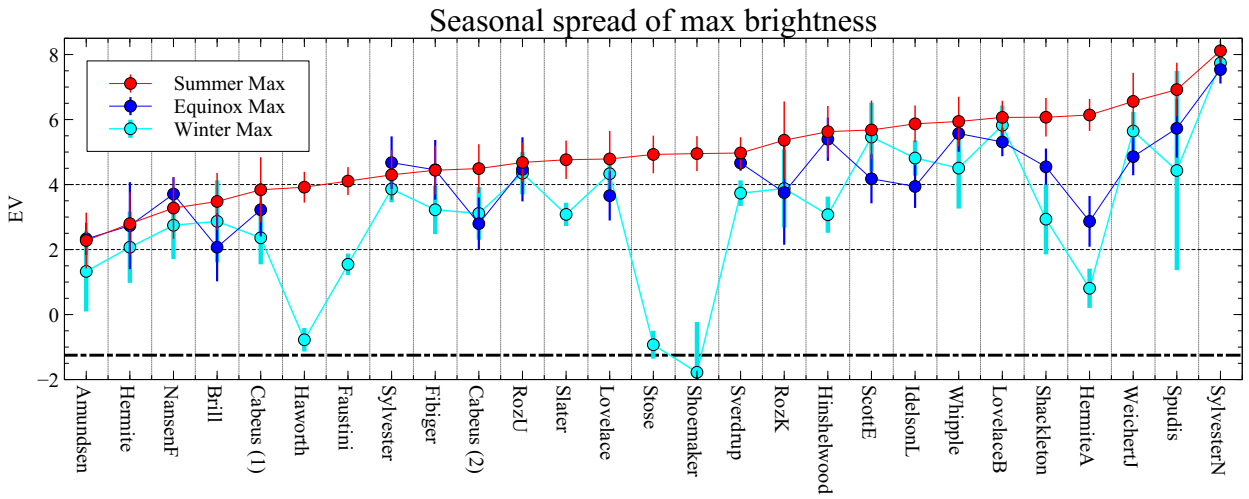

Figure 2: Variations in maximum observed brightness (of center test point) by crater and season (summer/winter: subsolar latitude poleward of ±1.0°; equinox: -0.5°<subsolar latitude<0.5°). The two Cabeus sites demonstrate variation within a large PSR (1 is near the LCROSS impact site, while 2 is 12 km east); interestingly, while their peak brightnesses differ by less than a factor of two, the time-of-day of peak brightness differs by ~1/5th of a month.

Photometric variation: Observed reflectance for a given location can vary considerably depending on photometric parameters, including lighting geometry, surface orientation, and observer position **[5]**. All of the observations studied here are nadir-looking, which will differ significantly from the brightness observed by an astronaut or camera on the surface. A full treatment of the photometry for any given image is beyond the scope of this work, as secondary light arrives from an immense number of angles, making detailed calculations complex for large datasets **[6]**. However, this complex integrated photometry can often be approximated by treating the incoming light as a point source, such as from the median source vector **[6]**, so for this work we approximate the lighting in PSRs as being from a single source at incidence angles of 60-90°, and determine adjustment factors for nadir-looking brightness with the empirical mature highlands LROC NAC photometric function from **[7]**. We calculated expected brightness for slopes from 0-30°, as seen from both an astronaut and ShadowCam.

Results: Maximum summer PSR brightnesses are frequently in ranges commonly found in well-lit buildings (**Fig. 2**), with the duration of near-maximum brightness typically being on the order of a week. Seasonal variation can be small or extreme, depending more on regional topography than size or latitude. Mean brightness of 600 m square patches varies by ± a factor of 2 within a few km, although variation within each patch is larger due to local bright slopes and shadows.

Photometry: Astronauts on the surface will see a full range of phase angles (angle between light source and observer) from 0° to 180°. Due to limits of the LROC NAC camera geometry, **[7]** is only valid from ~0-110° phase, but within those limits, the ratio of astronaut view/ShadowCam view for surfaces within 10 m ranges from ~0.3-5.0 (~±2 EV), with the lowest ratios being when the astronaut is facing towards the light source.

As a check on the photometric estimates, we also calculated the expected variation in brightness observed by ShadowCam between a level surface and a light-facing 30° slope. We found that the slope should have ~2-5× higher reflectance when viewed from overhead for incident light coming from 60-85° off-zenith, and indeed, ShadowCam images show slopes of small, crisp craters that are ~2-4× brighter than their surroundings.

Conclusions: Missions to PSRs will require careful evaluation of the lighting conditions for that specific site, but are unlikely to require artificial light except for detailed inspection of geologic samples.

Navigation towards the illuminated walls of PSRs may be challenging, both because the surface will appear dimmer due to photometric effects, and because the astronauts will have a large sunlit surface directly in their field of view. While traverses towards lit walls should be possible (similar to facing a wall of fluorescent office ceiling lights), they will likely be slower and less comfortable than in other directions within shadows (possibly similar to Apollo astronauts' experiences driving directly towards/away from the Sun).

References: **[1]** Robinson et al. (2023), *JASS*, 40(4):149-171. **[2]** Wagner et al (2024), 55th LPSC #2513. **[3]** Humm et al. (2023), *JASS*, 40(4):173-197. **[4]** ISO/CIE 23539:2023 (2023). **[5]** ISO 2720:1974 (1994). **[5]** Hapke (2012). Theory of Reflectance and Emittance Spectroscopy. **[6]** Martin et al. (2024), PSJ, 5:207 **[7]** Boyd et al. (2019), 50th LPSC #1992.